CHARACTERISATION OF CZT CRYSTALS FOR IMPROVED POSITION RESOLUTION AND DEFECT CORRECTION

UNIVERSITY OF LIVERPOOL

Emily E. Costello and Ellis Rintoul

sgecoste@Liverpool.ac.uk

Oliver Lodge Laboratory, University of Liverpool, Liverpool, L69 7ZE, U.K.

NuSec Nuclear Security Science Network

1 INTRODUCTION

Due to its excellent gamma ray spectral performance across a broad energy range and its ability to be operational at room temperature, CdZnTe (CZT) is a seemingly ideal candidate for applications in nuclear security. Despite these obvious advantages, today's commercial detector-grade CZT does not demonstrate a high level of material homogeneity. Through extended defects such as Te inclusions, grain boundaries, dislocations and twins, the performance and production of CZT is severely limited [1].

The requirement for high-grade detector crystals in industry limits the size of crystals that can be grown, meaning that for a high detector efficiency, a multi-element array of smaller crystals is necessary. However, these crystals must endure a pre-selection testing process, which further escalates costs. So, in terms of CZT's current industrial applications, it seems that one must accept either poor performance or high costs.

Five detector crystals of identical design and geometry were studied using precision collimated gamma scanning techniques. This allowed an investigation into the uniformity of response and areas of inhomogeneity within each crystal, as well as the identification of defects. Data taken and methods developed during this project could pave the way for the development of a detector-response correction, ultimately allowing for reduced CZT costs and increased efficiency.

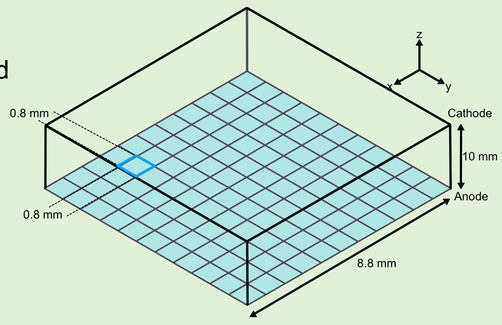

Schematic diagram of pixelized CZT detector crystal.

Each crystal has a 8.8×8.8×10 mm^3 volume; segmented into 11×11 pixels with 0.8 mm pitch.

The Kromek DMatrix Nuclear Imager (KDMNI) is a fully integrated, photon counting, pixelated, 12-bit energy discriminating CZT detector consisting a CZT detector module coupled to ASICs (which provide energy and timing information), ADC converters, and an FPGA [2].

2 DETECTOR CHARACTERISATION

DETECTOR LINEARITY

Sources with known γ emission energies were used (^{241}Am – 60keV, ^{57}Co – 122keV, ^{133}Ba – 80, 302, 356keV, ^{137}Cs – 662keV) and matched to their ADC channel number.

It can be seen that the detector response is linear and therefore required no further correction.

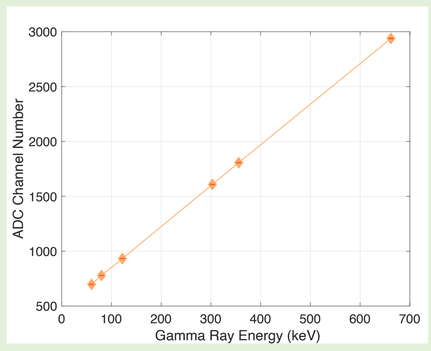

Detector characterisation measurements were performed with the ASIC readout to determine the optimal settings for further measurements across all five crystals.

Each characterisation measurement was taken using Crystal 1. All five crystals have identical design and geometry, hence the selected characterisation parameters could be used across all further spectra captured.

ENERGY RESOLUTION AS A FUNCTION OF BIAS VOLTAGE

Spectra were captured over a range of bias voltages, photopeaks were fitted and full width half maximums (FWHMs) calculated to quantify energy resolution.

The KDMNI has not yet been tested above 1600V, hence the voltage range was limited. The chosen setting was 1500V to optimise the detector response.

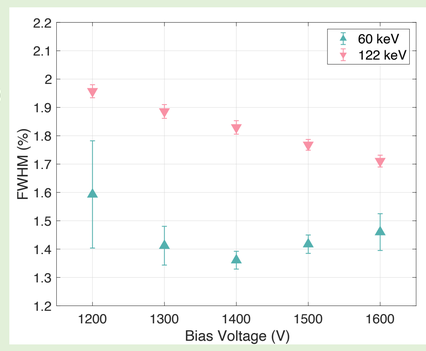

ENERGY RESOLUTION AS A FUNCTION OF PEAKING TIME

Spectra were captured over a range of peaking times, their photopeaks fitted and FWHMs calculated to quantify energy resolution. The KDMNI limited the range of peaking times to 2μs and below.

A peaking time of 2μs was selected in order to best reduce ballistic deficit [2] and FWHM.

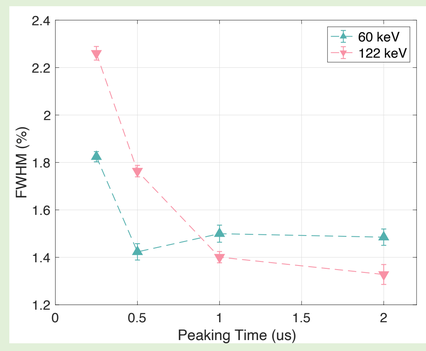

3 IDENTIFYING DEGRADED PIXELS AND CRYSTAL UNIFORMITY

A single detector crystal was placed into the Kromek DMatrix Nuclear Imager and spectra were captured with gamma sources of known emission energies (^{241}Am – 60keV, ^{57}Co – 122keV, ^{137}Cs – 662keV). The photopeaks were fitted and FWHMs were calculated, allowing one to plot FWHM uniformity maps of all 121 0.8x0.8 mm^2 pixels of the crystal. Using these, pixel spectra demonstrating low energy tailing and/or broadening could be identified for further investigation. Below are detector uniformity maps corresponding to ^{57}Co.

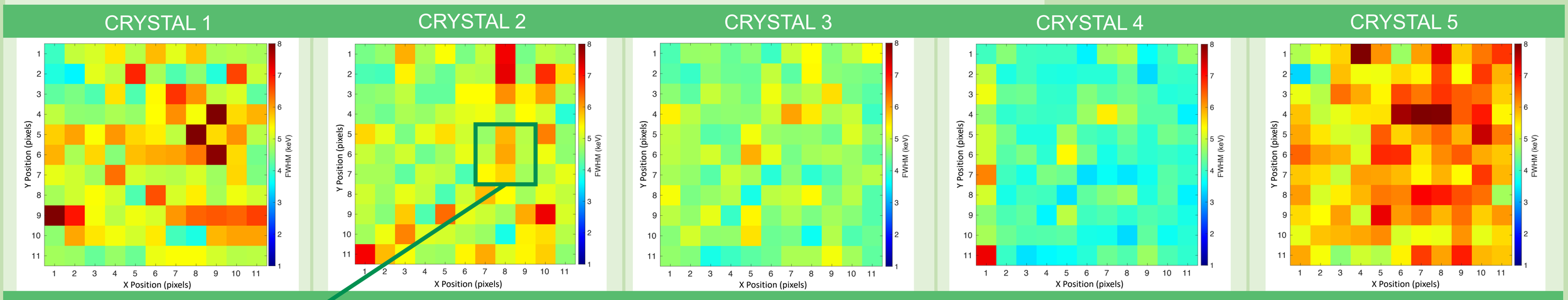

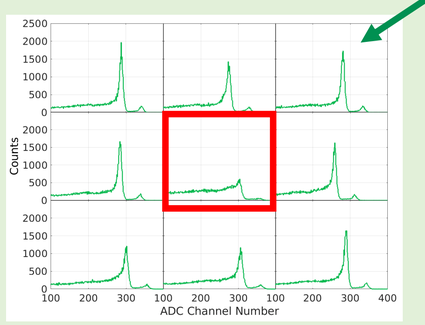

Pixel cluster 1 – a 3x3 cluster of raw pixel spectra located on detector Crystal 2.

In comparison to its neighbours, the central pixel in Pixel Cluster 1 highlighted on the left suffers significant charge loss, resulting in low energy tailing and a less defined photopeak.

One cause of this could be a Te inclusion which obstructs the electron cloud transportation through the crystal, resulting in a charge loss proportional to the number of electrons crossing this defect's geometrical area [3].

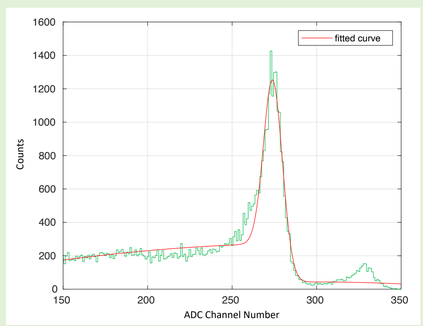

Photopeak with fitting function applied.

4 COLLIMATED SCANNING

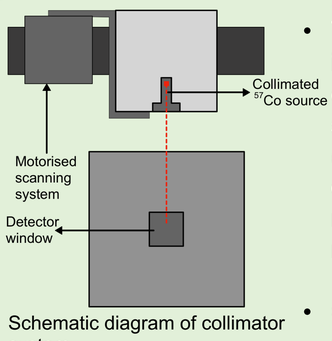

Schematic diagram of collimator system.

- The crystals were then separated from their ASIC stack and added into a digitizing system designed at the University of Liverpool, enabling signal readout of a 3x3 pixel cluster. Collimated gamma sources (^{241}Am, ^{57}Co, ^{137}Cs) were then attached to stepper motors (left) to gather charge collection and transient signals as a function of interaction position [4]. A 0.5 mm collimator was used to minimise beam divergence - a primary source of error in these measurements.
- On the right it is visible that, for collimator positions within the area of a defect, there are fewer full photopeak counts. This effect can be studied further in the spectra below, where it becomes apparent that charge loss is the cause of this. Similarly, further into the defect, the average photopeak energy begins to shift lower – this effect can be used in the development of a correction method.

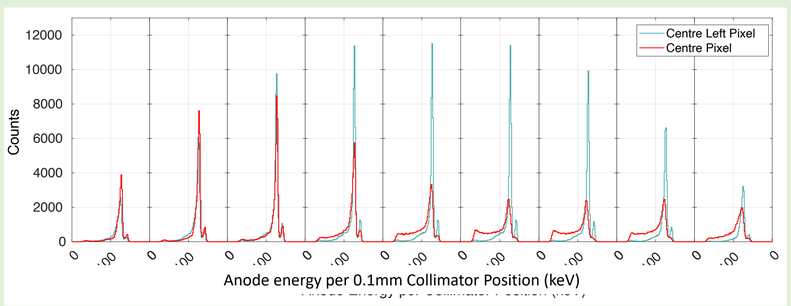

Comparison of energy spectra using ^{57}Co as a function of collimator position across the widths of the centre left and centre pixel in pixel cluster 1 located on crystal 2.

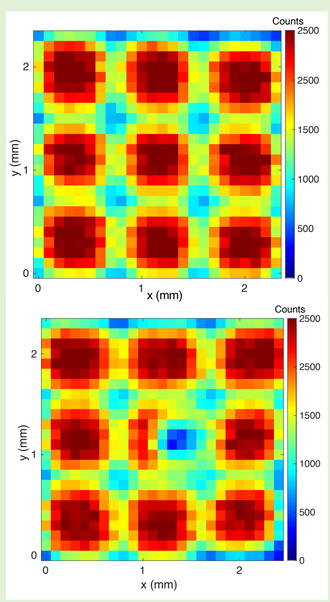

Comparison of typical cluster from crystal 4 (top) to degraded cluster from crystal 2 (bottom) intensity maps showing number of full photopeak events as a function of collimator position.

5 PULSE SHAPE ANALYSIS

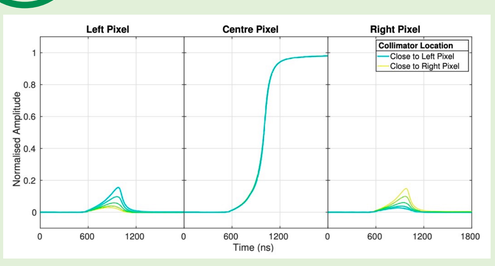

Left: average charge collection signal and neighbouring transient image charges for 5 collimator positions across a central pixel [4].

- Digital readout signals from the collimator system designed at the University of Liverpool allow the output of average signals across collimator position. Due to their position dependence, the ratio between neighbouring image charge signals can be parameterised to give an indication of defect position.

$$A = \frac{Q_A - Q_B}{Q_A + Q_B}$$

Where Q_A and Q_B are net areas of opposing image charges.

- These asymmetry parameters can then be used to determine the position of gamma interactions without the need for collimated position information. This methodology has been used to achieve sub-pixel position resolution [4].
- Spectra were created and compared across the 0.8 mm pixel width based upon the known-collimator position and the PSA-determined position. Below, it's visible that these PSA approximations reflect collimated spectra well, and therefore these methods could be used to develop a defect correction method.

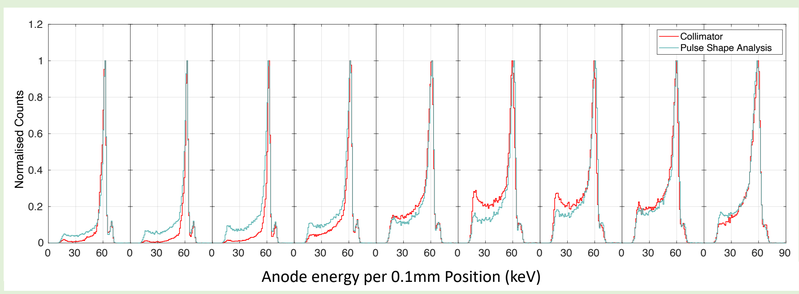

Normalised counts across 0.8mm pixel width based upon PSA-determined and collimator-determined positions.

6 FUTURE WORK

- Collimated side scans of the detector have been performed to quantify detector response as a function of depth of interaction. This will allow position resolution improvement and defect correction through the 10mm depth of the detector using rise time analysis.
- Data has been taken for multiple degraded clusters at a range of energies to be used in the development and implementation of a universal defect correction method, improving the suitability of CZT detector crystals for nuclear security applications.

REFERENCES

[1] Bolotnikov, A., & al., 2010. Te Inclusions in CZT Detectors: New Method for Correcting their Adverse Effects. *IEEE Transactions on Nuclear Science,* April, 57(2), pp. 910-919.
[2] McAreavey, L. & al., 2017. Characterisation of a CZT detector for dosimetry of molecular radiotherapy. *Journal of Instrumentation,* Volume 12.
[3] Bolotnikov, A.E, & al., 2013. Characterisation and evaluation of extended defects in CZT crystals for gamma-ray detectors. *Journal of Crystal Growth,* Volume 379, pp. 46-56.
[4] Rintoul, E., & al., 2022. Sub-Voxel Identification of Gamma-Ray Interaction Positions within a Pixelated CZT Detector through Signal Analysis. *In Review.*